

Bipartite Graph Variational Auto-Encoder with Fair Latent Representation to Account for Sampling Bias in Ecological Networks

Emre Anakok¹, Pierre Barbillon², Colin Fontaine³, and Elisa Thebault⁴

^{1,2} *Université Paris-Saclay, AgroParisTech, INRAE, UMR MIA Paris-Saclay, 91120, Palaiseau, France.*

³ *Centre d'Écologie et des Sciences de la Conservation, MNHN, CNRS, SU, 43 rue Buffon, 75005 Paris, France*

⁴ *Sorbonne Université, CNRS, IRD, INRAE, Université Paris Est Créteil, Université Paris Cité, Institute of Ecology and Environmental Sciences (iEES-Paris), 75005 Paris, France*

¹ *emre.anakok@agroparistech.fr*

Abstract

We propose a method to represent bipartite networks using graph embeddings tailored to tackle the challenges of studying ecological networks, such as the ones linking plants and pollinators, where many covariates need to be accounted for, in particular to control for sampling bias. We adapt the variational graph auto-encoder approach to the bipartite case, which enables us to generate embeddings in a latent space where the two sets of nodes are positioned based on their probability of connection. We translate the fairness framework commonly considered in sociology in order to address sampling bias in ecology. By incorporating the Hilbert-Schmidt independence criterion (HSIC) as an additional penalty term in the loss we optimize, we ensure that the structure of the latent space is independent of continuous variables, which are related to the sampling process. Finally, we show how our approach can change our understanding of ecological networks when applied to the Spipoll data set, a citizen science monitoring program of plant-pollinator interactions to which many observers contribute, making it prone to sampling bias.

1 Introduction

1.1 Context

Graph embedding regroups different methods, allowing to represent a network into a vector space in order to gain understanding of key network features. These methods are especially important in the context of large networks. Recently developed graph neural networks (GNNs) enable graph embedding with large-scale methods such as graph isomorphism network (Xu et al., 2019), graph attention network (Veličković et al., 2018) or the variational graph variational auto-encoder (Kipf and Welling, 2016). All these methods can also handle numerous covariates on nodes. GNNs are currently growing in popularity in various domains such as bioinformatics (Zhang et al., 2021) and chemistry (Reiser et al., 2022), but they remain mostly unknown in other research fields.

In ecology, networks have been analyzed to study various types of interaction between species of plants and animals (Ings, 2009). The stochastic block model (Nowicki and Snijders, 2001) and the latent block model (Govaert and Nadif, 2010) for bipartite graphs are notorious models using

latent variable in ecology (Terry and Lewis, 2020; Durand-Bessart et al., 2023). While graph embedding methods start being used for ecological networks (e.g. Botella et al. (2022), Strydom et al. (2022)), GNNs have yet to be diffused in that research field. GNNs could be particularly relevant for ecological networks because very large data sets of interactions among species are now becoming available (e.g. through the development of citizen science programs), in addition to many covariates linked to the nodes (e.g. species name and traits, environmental characteristics at the time of interaction observation).

An important issue with the analysis of ecological networks is related with the strong effects of sampling effort and methods on network structure (Jordano, 2016; Doré et al., 2021). Sampling interactions among species to build ecological networks is indeed a daunting task. For example, extensive sampling of plant-pollinator interactions has been shown to only provide a subset of the existing interactions (Chacoff et al., 2012; Jordano, 2016) and sampling protocols are known to be subject to bias (Gibson et al., 2011), both of which need to be accounted for to make meaningful ecological interpretations (Doré et al., 2021). One could wish to have an embedding which is independent of a certain set of covariates linked to such sampling effects and related bias. This can be of particular interest for citizen science programs, where biases can arise from the observer’s experience level (Jiguet, 2009; Deguines et al., 2018).

The solution to correct for sampling biases in ecological network analysis may be found in machine learning applied to sociology with the notion of fairness (Caton and Haas, 2020; Carey and Wu, 2022), where the main idea is to train an algorithm whose predictions are independent of a protected variable. It is used in sociology (Carey and Wu, 2022) to have prediction that are independent of gender, sexuality or disability. Recently, works on fairness have been extended to social network analysis (Saxena et al., 2022), for fair link prediction (Li et al., 2021), fair graph exploration (Rahman et al., 2019) or other network characteristic. Fairness has also been developed for variational auto-encoder, with the fair auto-encoder (Louizos et al., 2017) or with adversarial debiasing (Zhang et al., 2018), which can help to aim for a fair latent representation of the network. Most papers about fairness for network seeks for fairness regarding a binary (or a categorical) protected variable (Saxena et al., 2022) which is not always appropriate to the study of ecological networks where sampling biases might also be measured by continuous variables (e.g. sampling time, observer’s experience level). The adversarial debiasing from Zhang et al. (2018) could be applied to continuous variables, but has theoretical guarantees for the discrete protected variable. Even if the fair variational auto-encoder (Louizos et al., 2017) assumes independent prior, they penalize their loss with a regularization term that considers a discrete protected variable.

Another domain of machine learning that can provide interesting literature is recommender systems (Beel et al., 2016; Li et al., 2023). The main task of a recommender system is to predict the preference scores of users over items so that the model can recommend each user a top-N recommendation list. This can be useful if the goal is to predict for a given plant species the top-N insect which are going to pollinate it. However, in ecological studies, plant species can be either specialists with few or none pollinator interactions or generalists with many interactions. Predicting the overall visitation network is thus a different task from predicting the specific top-N pollinators for each plant species. Recommender systems nonetheless provide literature about fairness for different characteristics on graphs with heterogeneous nodes (Li et al., 2023; Wang et al., 2023), but the protected variable is also binary or categorical. Moreover, the targeted fairness in recommender systems is not adapted to address sample bias in ecology since the former focus on ensuring equitable recommendations for users (Li et al., 2023), which is a user-centric goal, while the latter deals with a broader scope of the whole network.

There are other machine learning methods related with debiasing taking account continuous variables, such as disentanglement methods. For example the $\beta - VAE$ (Higgins et al., 2016) can

provide a latent space with some conditionally independent latent factors. However their goal is different because they do not seek complete independence between the latent representation and the sensitive factors (Locatello et al., 2019).

Gretton et al. (2005) presented the Hilbert-Schmidt independence criterion as a measure of independence between two random variables. It can be used as a penalty term to ensure independence between continuous variable. This metric has been put in practice in learning context by Greenfeld and Shalit (2020) or Ma et al. (2020). It can be estimated and its estimation can be associated with a statistical test of independence Gretton et al. (2007). As fairness deals with independence of protected variables, it can be useful to consider the HSIC in this context.

In this paper, we aim to obtain a latent representation of our ecological network that is independent of covariates that may be continuous. First, we specify our goal in a simple context where linear embeddings are considered with a simple data structure. After presenting the necessary background on GNNs and the HSIC criterion, we introduce the model. We attest the performance of our proposed model with simulated data. Finally, we apply our methodology to the Spipoll data set (Deguines et al., 2012), a citizen science program monitoring plant-pollinator interactions across France since 2010, where we show that accounting for the sampling effort can change the understanding of the network.

1.2 The linear embedding case

It is difficult to consider a fairness problem in the network framework because of the structure of the data itself. Ensuring fairness in network analysis involves addressing disparities in the representation and impact of the connection pattern and the covariates available. To have a better understanding of the problem at stake, we first present the available tools when we consider a linear embedding for a dataset living in a real linear space.

Let X a $n \times d$ matrix and let S be $n \times d_s$ matrix. Without loss of generality, we assume that each column of X has been centered. We wish to perform a one dimensional principal component analysis on X that would yield us a vector v and a lower dimensional embedding of X given by Xv that maximizes the variance. However, we wish to have a latent representation Xv independent of the protected variable S . If we were in the context of probabilistic PCA (Tipping and Bishop, 1999) where X and S would have been multivariate Gaussian, projecting X onto the space orthogonal to S : S^\perp beforehand would have been enough to guarantee the independence between S and the latent representation Xv , this can be solved using PPCA with covariates (Kalaitzis and Lawrence, 2012).

We show that this approach is equivalent to find the optimal projection with respect to an independence constraint.

Proposition 1 Assume that X is centered. Let $\Lambda = \frac{1}{n}X^\top X$. Assume that X and S are jointly Gaussian. The solution of the maximization problem given by the following Lagrangian:

$$L(v) = v^\top \Lambda v + \lambda_1(1 - v^\top v) + \lambda_2 \|S^\top Xv\|^2 \quad (1)$$

can also be obtained by computing the first component of the PCA of $P_{S^\perp} X$. Proof of the proposition can be found in the supplementary material.

2 Background

We have reformulated the linear embedding problem under independence constraint as an optimization problem with a supplementary term that encourages the independence. This

optimization formulation can be used for graph network analysis. Embedding the graph as a vector using a variational graph auto-encoder (VGAE) (Kipf and Welling, 2016) would yield a Gaussian latent representation Z . As we cannot guarantee that Z and S are jointly Gaussian, we will use another criterion than the covariance to have independence between Z and S : the Hilbert-Schmidt independence criterion (HSIC), first proposed by Gretton et al. (2005) which is a metric testing for the independence of two variables. Compared to the other proposed methods of embedding, the probabilistic setting of the GVAE fits well with the use of the HSIC, and its generative aspect allows network generation for various ecological contexts.

2.1 Bipartite variational graph auto-encoder

We adapt the variational graph auto-encoder from Kipf and Welling (2016) to the bipartite case by considering two graph convolutional networks (GCN), one for each node types.

We consider a biadjacency matrix $B_{i,j}$ of size $n_1 \times n_2$ representing our graph. Let

$$D_1 = \text{diag} \left(\sum_{j=1}^{n_2} B_{i,j} \right) \quad D_2 = \text{diag} \left(\sum_{i=1}^{n_1} B_{i,j} \right)$$

be respectively the row and the column degree matrices. For each i and each j we consider the stochastic latent variables Z_{1i} and Z_{2j} which are described respectively by a $n_1 \times D$ and a $n_2 \times D$ matrices (they share the same number of columns). X_1 is a $n_1 \times d_1$ matrix of node features for the first category, and X_2 is a $n_2 \times d_2$ matrix of node features for the second. Finally, we consider the normalized biadjacency matrix $\tilde{B} = D_1^{-\frac{1}{2}} B D_2^{-\frac{1}{2}}$.

2.1.1 Encoder

Our encoder is defined as

$$q(Z_1, Z_2 | X_1, X_2, B) = \prod_{i=1}^{n_1} q_1(z_{1i} | X_1, B) \prod_{j=1}^{n_2} q_2(z_{2j} | X_2, B)$$

with

$$q_v(z_{vi} | X_v, B) = \mathcal{N}(\mu_{v,i}, \text{diag}(\sigma_{v,i}^2)), \quad v \in \{1, 2\}$$

with μ_v and $\log(\sigma_v)$ obtained by the GCN_v defined similarly as Kipf and Welling (2016):

$$\begin{aligned} \text{GCN}_1(X_1, B) &= \tilde{B} \text{ReLU}(\tilde{B}^\top X_1 W_{1,1}) W_{1,2} \\ \text{GCN}_2(X_2, B) &= \tilde{B}^\top \text{ReLU}(\tilde{B} X_2 W_{2,1}) W_{2,2} \end{aligned}$$

with weight matrices W_v . $\text{GCN}_{\mu_v}(X_v, B)$ and $\text{GCN}_{\sigma_v}(X_v, B)$ share the first-layer parameters $W_{v,1}$ and $\text{ReLU}(x) = \max(x, 0)$.

2.1.2 Decoder

Our decoder is defined as

$$p(B | Z_1, Z_2) = \prod_{i=1}^{n_1} \prod_{j=1}^{n_2} p(B_{i,j} | z_{1i}, z_{2j})$$

with

$$p(B_{i,j}|z_{1i}, z_{2j}) = e^{-\frac{\|z_{1i}-z_{2j}\|^2}{2\sigma^2}}.$$

For the rest of the paper, we have considered $\sigma^2 = 1$ for the decoder.

The full auto-encoder can be summarized as

$$B, X_1, X_2 \xrightarrow[\text{encoder}]{q(Z_1, Z_2|X_1, X_2, B)} Z_1, Z_2 \xrightarrow[\text{decoder}]{p(B|Z_1, Z_2)} \widehat{B}.$$

2.2 Hilbert Schmidt Independence Criterion

2.2.1 Definition

Let X and Y two random variables in \mathcal{X} and \mathcal{Y} and (X, Y) be the joint probability distribution. Let \mathcal{F} and \mathcal{G} be the RKHS on \mathcal{X} and \mathcal{Y} with their associated kernel $K : \mathcal{X} \times \mathcal{X} \rightarrow \mathbb{R}$ and $L : \mathcal{Y} \times \mathcal{Y} \rightarrow \mathbb{R}$. [Gretton et al. \(2005\)](#) define the HSIC as the norm of the cross-variance operator between the distribution in the RKHS:

$$\begin{aligned} HSIC(X, Y) &= \|C_{X,Y}\|^2 \\ &= \mathbb{E}_{X,Y,X',Y'}[K(X, X')L(Y, Y')] \\ &\quad + \mathbb{E}_{X,X'}[K(X, X')]\mathbb{E}_{Y,Y'}[L(Y, Y')] \\ &\quad - 2\mathbb{E}_{X,Y}[\mathbb{E}_{X'}[K(X, X')]\mathbb{E}_{Y'}[L(Y, Y')]]. \end{aligned}$$

Using some specific kernels such as the Gaussian kernel $K(x_i, x_j) = e^{-\frac{\|x_i-x_j\|^2}{2\sigma^2}}$ it can be shown that $HSIC(X, Y) = 0 \iff X \perp Y$ ([Gretton et al., 2005](#)).

2.2.2 Estimation

Given $(x_1, y_1) \dots (x_n, y_n)$ an i.i.d. sample drawn from (X, Y) , and given the corresponding evaluations of the two kernels $K_{ij} = K(x_i, x_j)$ and $L_{i,j} = L(y_i, y_j)$, a biased estimator of the HSIC is given by

$$\begin{aligned} \widehat{HSIC} &:= \widehat{HSIC}(\{(x_i, y_i)\}_{i=1}^n) \\ &= \frac{1}{n^2} \sum_{1 \leq i, j \leq n} K_{i,j} L_{i,j} + \frac{1}{n^4} \sum_{1 \leq i, j, p, q \leq n} K_{i,j} L_{p,q} \\ &\quad - \frac{2}{n^3} \sum_{1 \leq i, j, q \leq n} K_{i,j} L_{i,q}. \end{aligned} \tag{2}$$

Under the assumption that X and Y are independent, it has been proved that the distribution of $n \times \widehat{HSIC}$ can be asymptotically approximated by a Gamma distribution ([Gretton et al., 2007](#))

$$n \times \widehat{HSIC} \sim \frac{x^{\alpha-1} e^{-\frac{x}{\beta}}}{\beta^\alpha \Gamma(\alpha)}$$

where $\alpha = \frac{\mathbb{E}[\widehat{HSIC}]^2}{\mathbb{V}[\widehat{HSIC}]}$ and $\beta = \frac{n\mathbb{V}[\widehat{HSIC}]}{\mathbb{E}[\widehat{HSIC}]}$.

During the learning phase, using the HSIC as a penalty between the coordinates in the latent space and the protected variable will assure that the latent space is as much as possible

independent of the protected variable. At the end of the learning, we can check the independence by calculating the p-value of the test and compare it to the desired significance level. An example in the linear case is available in Appendix B.3.

2.3 Estimation in high dimension

Calculating \widehat{HSIC} requires to compute the $n \times n$ Gram matrix and can be time-consuming for large value of n . As a substitute, we can use Random Fourier Features (RFF) (Rahimi and Recht, 2007). RFF for learning has been used in (Louizos et al., 2017) to minimize the maximum mean discrepancy (MMD) between two distributions, in a setting where the protected variable have two possible values. Using the Gaussian kernel, minimizing the MMD is equivalent to matching all the moments of the two distribution, making the outcome of the encoder fair. In our settings, the HSIC can be seen as the MMD between the joint distribution (X, Y) and the product of the distribution X and Y . If the joint distribution is close to the product of the two distribution then the X and Y will behave as they are independent.

Assume that $K(x_i, x_j) = e^{-\frac{1}{2}\|x_i - x_j\|^2}$ ($\sigma^2 = 1$), with $x_i \in \mathbb{R}^d$, let $D < n$, ω be a $D \times d$ matrix where all entries are independently drawn from $\mathcal{N}(0, 1)$ and b be d -dimensional vector with each entry independently drawn from $Unif([0, 2\pi])$. For any x_i , its RFF is defined as

$$\psi_X(x_i) = \sqrt{\frac{2}{D}} \cos(\omega x_i^\top + b) \in \mathbb{R}^D.$$

The main idea behind this RFF representation is that $K(x_i, x_j) \approx \langle \psi_X(x_i), \psi_X(x_j) \rangle$, this property will allow the computation to be much faster, while having a small error term (Sutherland and Schneider, 2015). If we also define ψ_Y the as RFF of Y , then finally we can estimate the RFF HSIC (Zhang et al., 2018) as:

$$RFF\ HSIC = \frac{1}{n^2} \left\| \sum_{i=1}^n \psi_X(x_i) \psi_Y(y_i)^\top - \frac{1}{n} \left(\sum_{i=1}^n \psi_X(x_i) \right) \left(\sum_{i=1}^n \psi_Y(y_i) \right)^\top \right\|_2^2.$$

The RFF HSIC can then be computed accurately with complexity $O(D^2)$. Several other methods of estimation for HSIC exists for large-scale problem (Zhang et al., 2018). For the rest of this paper, $D = 100$ will provide enough accuracy.

3 Bipartite and fair graph variational auto-encoder

Suppose our goal is to construct the latent representation Z_1 of the bipartite variational auto-encoder such as it is independent of a protected variable denoted by S . We optimize our parameters W_i to minimize a compromise between the variationnal lower bound of the auto-encoder and the HSIC between μ_1 and the protected variable S . Even if the reconstruction would be penalized, this would yield a latent-space $\tilde{Z}_1 \sim \mathcal{N}(\mu_1, \text{diag}(\sigma_1^2))$ independent of S . The complete loss of this

auto-encoder can be written as:

$$\begin{aligned}
L = & \mathbb{E}_{q(Z_1, Z_2 | X_1, X_2, B)} [\log p(B | Z_1, Z_2)] \\
& - KL[q_1(Z_1 | X_1, B) || p_1(Z_1)] \\
& - KL[q_2(Z_2 | X_2, B) || p_2(Z_2)] \\
& + \delta RFF HSIC(\mu_1, S)
\end{aligned} \tag{3}$$

where δ is a hyperparameter, KL is the Kullback-Leibler divergence, and p_1, p_2 are Gaussian priors for Z_1 and Z_2 . This method can also be extended to the case where we also seek independence between Z_2 and another protected variable.

4 Simulation

4.1 Setting

In this simulation, we are going to generate bipartite networks made of $n_1 = 1000$ rows and $n_2 = 100$ columns. Let $S_i \stackrel{i.i.d.}{\sim} \mathcal{N}(0, 1)$ for $i = 1, \dots, n_1$ and $T_i \stackrel{i.i.d.}{\sim} \mathcal{N}(0, 1)$ for $i = 1, \dots, n_1$ and independent of S . We suppose that S is the protected variable. Let $Z_1 = (S, T) \in \mathbb{R}^{n_1 \times 2}$ be the 2-column matrix made with both S and T . Let $Z_2 \stackrel{i.i.d.}{\sim} \mathcal{N}\left(\begin{bmatrix} 2.5 \\ 2.5 \end{bmatrix}, \begin{bmatrix} 1 & 0 \\ 0 & 1 \end{bmatrix}\right) \in \mathbb{R}^{n_2 \times 2}$. We simulate our bipartite adjacency matrix with a Bernoulli distribution $B_{i,j} \stackrel{i.i.d.}{\sim} \mathcal{B}(\exp(-\frac{1}{2} \|Z_{1i} - Z_{2j}\|_2^2))$.

First, we fit a classical bipartite and variational graph auto-encoder on $B_{i,j}$. We expect that this auto-encoder would yield a latent representation \tilde{Z}_1 correlated with S and T . We then fit our bipartite and fair auto-encoder to compare the result and see if the yielded latent space is independent of S . We also compare our methodology with an adversarial learning algorithm (ADV) (Zhang et al., 2018) where the output μ_1 is then used as an input to a 4-layer perceptron which attempts to predict the protected variable S . The loss is then penalized if the predicted output is correlated with the protected variable. As explained in the introduction, it is the only contender we identified to achieve fairness for a continuous protected variable.

4.2 Results

The results for the link prediction task in the simulated network are summarized in Table 1. The simulations were done with dataset splits, with 30% of the edges hidden. 20% of these hidden edges are used as validation data set, and the remaining 10% for the test set. Both sets also contain an equivalent amount of non-edges that are not in the train set. We compare the methods with the area under the ROC curve (AUC) score, the average precision (AP) score, the *HSIC* between the latent space \tilde{Z}_1 and S , the number of times the p-value associated with the *HSIC* Independence test is lower than 0.05% ($\#p_{0.05}$) and the Euclidean norm of the correlation matrix between \tilde{Z}_1 and S (*cor*). In the table, are reported the mean and standard deviation for 100 trials, except for $\#p_{0.05}$ which is only a count. We set the hyperparameter $\delta = n_1$. For each trial, the simulations begin with 10 random initializations, and were fit using 1000 iterations of the Adam algorithm with learning rate 0.01, using a computer equipped with an Intel Xeon(R) CPU E5-1650 v4 and 32GB of RAM. The model that achieved the most favorable performance on the validation test set is then selected to evaluate the performance on the test dataset.

As we expected, the AUC and AP for link prediction decreases when we penalized the reconstruction with the *HSIC*, because in our setting, nodes with higher value for S should have a higher probability of connection. However, the latent space given by the BVGAE is not

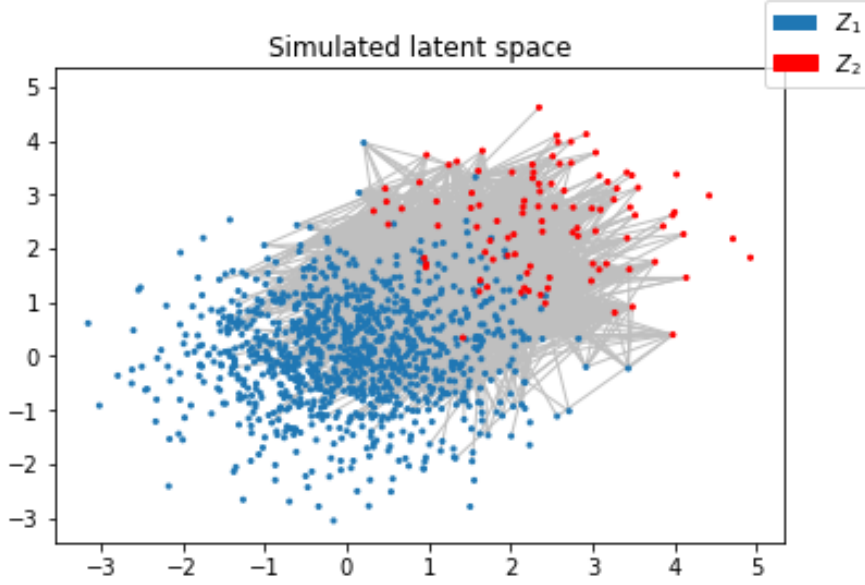


Figure 1: Simulated latent space for generating bipartite network $B_{i,j}$. $Z_1 = (S, T)$ is represented in blue. Z_2 is represented in red and is independent of Z_1 . The probability of connection between the node i and j will increase as the distance between their latent representation decreases.

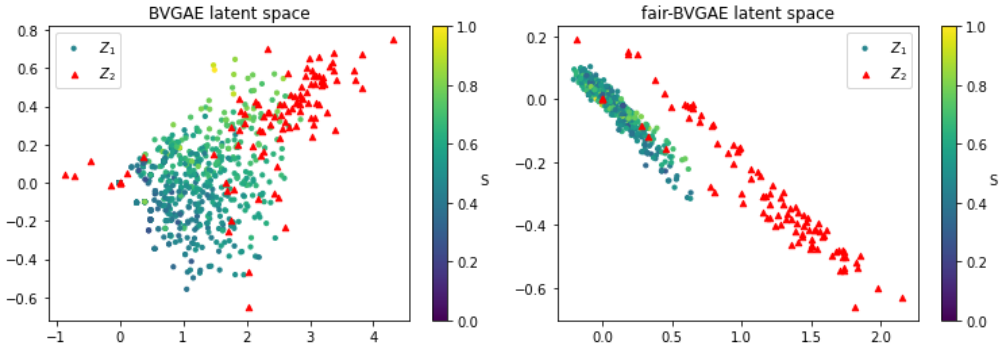


Figure 2: Estimated latent space for the bipartite variational graph auto-encoder (left) and the fair bipartite variational graph auto-encoder (right).

independent of the protected variable S . This can be seen by looking at the p-value of the HSIC Independence test and the correlation between \tilde{Z}_1 and S . Even if it is not enough to guarantee independence, we can see that the correlation between the latent space and the protected variable is much higher in the BVGAE than in the fair-BVGAE and ADV model. However, in all the simulations, the independence hypothesis has been rejected for the BVGAE and kept for the fair-BVGAE. The ADV model managed to have a smaller HSIC than the BVGAE, however the independence hypothesis was rejected most of the time. The ADV model is much harder to calibrate because it requires a second neural network to optimize.

An example of the latent space of BVGAE and fair-BVGAE can be seen in figure 2. Looking at the coloring, we can see for the BVGAE that the latent space is clearly correlated with S ,

Table 1: Comparison between the Bipartite variational graph auto-encoder and its fair counterparts on 100 trials with simulated data.

	BVGAE	fair-BVGAE	ADV
AUC	0.894 ± 0.013	0.835 ± 0.024	0.702 ± 0.0523
AP	0.879 ± 0.017	0.805 ± 0.030	0.685 ± 0.0570
HSIC	0.022 ± 0.005	8.70×10^{-6} $\pm 5.04 \times 10^{-6}$	5.82×10^{-3} ± 0.00501
# $p_{0.05}$	100/100	0/100	99/100
<i>cor</i>	0.753 ± 0.095	0.043 ± 0.035	0.263 ± 0.187

while the latent space of the fair-BVGAE does not share structure with the protected variable S . The HSIC test between the fair latent space and S yields us a p-value equals to 0.139, we do not reject the hypothesis that the latent space Z_1 is independent of S . Simulation with binary protected variable is available in Appendix B.2.

5 Application on the Spipoll data set

5.1 Context

We evaluate our methodology on the Spipoll (Deguines et al., 2012) data set, a French citizen science program aiming at monitoring plant-pollinator interactions across metropolitan France since 2010. This monitoring follows a simple protocol: briefly, volunteers can choose a flowering plant where and when they like, and during 20 minutes, take pictures of all different insects that land on the flowers of the monitored plant. Then, using an online identification tool, they identify each different insect that has been photographed and upload their data on a dedicated website. Each participation is thus a set of insect interactions with a given plant species that have been observed at a given time and place, and by a given volunteer whose specific skills could affect the quality of the observation. The date and place of observations allowed us to extract corresponding climatic conditions as covariates, from the European Copernicus Climate data set provided by Cornes et al. (2018).

A common practice in ecology to study plant-pollinator interactions is to consider plant and insect species as nodes of a bipartite network, with edges determined by the interactions observed between the two. In the case of Spipoll data set, this implies aggregating all observations of the interactions between a given plant and insect species, and all the covariates describing observation conditions, such as date and climate should be aggregated accordingly. However, the way to perform such aggregation is not straightforward. Therefore, we wish to change paradigm and to consider a bipartite network where the first type of nodes are session of observations, and the second type are insects observed during the session. Each session has the previously mentioned covariates and a one-hot encoding describing the plant genus. This paradigm allows us to directly use the Spipoll data without having to do any aggregation at all. Link prediction task in this situation aims to predict which insect will be present during a given the observation session. However, we still wish to ultimately obtain a bipartite plant-insect network, as this is the most widely used tool in this field of study. To ensure that the latent space could also be used to create a plant-insect network, we propose to draw for each taxon of plant one observation from the set of all the session where this plant was monitored. This would generate a plant-insect latent space

Z'_1, Z_2 , and using the same decoder, would generate a plant-insect network.

While citizen science programs facilitate the accumulation of observed data, the sampled data may be biased by the participating observers. In the Spipoll dataset, [Deguines et al. \(2018\)](#) have reported that the accuracy of insect taxa identification increases with higher level of user participation. Similarly, [Jiguet \(2009\)](#) found in a breeding bird survey that observers tended to count more birds after the first year compared to the initial year of observation. In order to mitigate the bias introduced by the observers, [Johnston et al. \(2018\)](#) suggested estimating the observers' expertise and incorporate it as a covariate in their model. In the context of the Spipoll dataset, [Deguines et al. \(2016\)](#) addressed the potential variation in the number of photographed insects among different observers by incorporating observer identity as a random term in their model's intercept.

We propose in our setting to define S , the protected variable, as the number of participation from the user. This number of participation would work as a proxy of the user's experience. By employing this measure, we aim to construct a latent space that remains unaffected by variations in observers' experience levels.

5.2 Model

In this part, we elaborate on the application of our methodology, taking into account the specific requirements of the Spipoll data set. We consider B our $n_1 \times n_2$ incidence matrix, where the n_1 rows correspond to the number of sampling session, and the n_2 columns correspond to the number of different observed pollinators in the dataset. For all i and j , $B_{i,j} \in \{0, 1\}$ describes the absence or the presence of the pollinator j during the session i . Let $P = (P_{i,k})$, $i = 1, \dots, n_1, k = 1, \dots, u$ where u correspond to the number of observed taxa of plants. $P_{i,k} \in \{0, 1\}$ is a binarized categorical variable which describes the plant taxonomy of the i^{th} session. For all i , there is only one coordinates k such that $P_{i,k} = 1$ while the others are equal to 0. To build the binary adjacency matrix B' of plant-pollinator interaction from the session-pollinator matrix B , we compute $B' = \mathbf{1}(P^\top B > 0)$. We create the second latent space after one realization of the first:

$$\tilde{q}(Z'_1|Z_1, P) = \prod_{l=1}^u q_1(z'_{1l}|Z_1, P)$$

where for any l , $q_1(z'_{1l}|Z_1, P)$ samples uniformly one Z_{1i} among the one where $P_{i,l} = 1$. We use the same decoder for both latent space. Let

$$\tilde{P}_{i,k} = \frac{P_{i,k}}{\sum_{l=1}^{n_1} P_{l,k}}.$$

It is also possible to estimate B' from the reconstruction \hat{B} itself, by calculating $\hat{B}' = \tilde{P}^\top \hat{B}$. This is equivalent to calculate the mean by plants of the predicted probabilities of interaction. The model is summarized with the following scheme:

$$\begin{array}{ccccc} B, X_1, X_2 & \xrightarrow{q} & Z_1, Z_2 & \xrightarrow{p} & \hat{B} \\ \downarrow \mathbf{1}(P^\top B > 0) & & \downarrow \tilde{q} & & \downarrow \tilde{P}^\top \hat{B} \\ B' & & Z'_1, Z_2 & \xrightarrow{p} & \hat{B}' \end{array}$$

The protected variable S is the log base 10 of the number of observation session the user has already performed. To fit this model, we minimize the same loss as [3](#) with a supplementary term

$$L' = L + \mathbb{E}_{\tilde{q}(Z'_1, Z_2|X_1, X_2, B, P)}[\log p(B'|Z'_1, Z_2)].$$

5.3 Results

Table 2: Comparison between the Bipartite variational graph auto-encoder and its fair counterpart on 10 trials on the Spipoll data set.

	BVGAE	fair-BVGAE
AUC1	0.865 ± 0.003	0.830 ± 0.005
AP1	0.855 ± 0.003	0.825 ± 0.005
AUC2	0.730 ± 0.017	0.712 ± 0.022
AP2	0.725 ± 0.022	0.710 ± 0.026
AUC3	0.756 ± 0.020	0.728 ± 0.019
AP3	0.751 ± 0.022	0.724 ± 0.024
HSIC	2.21×10^{-4} $\pm 0.15 \times 10^{-4}$	5.38×10^{-7} $\pm 2.83 \times 10^{-7}$
# $p_{0.05}$	10/10	0/10
<i>cor</i>	0.051 ± 0.004	0.004 ± 0.002

We consider the observation period of the Spipoll data set from 2017 to 2020 included in metropolitan France and Belgium. We consider a total of $n_1 = 12754$ of observation session, where $n_2 = 306$ taxa of insects and $u = 83$ genus of plants have been observed. The observation session-insect matrix B has a total of 94 909 interactions reported, and the plant-insect matrix B' has 9 754 different interactions. The results for the link prediction task for the Spipoll data set are summarized in Table 2. The predictions were made with the complete dataset B , that has been split with 30% of the edges hidden. 20% of these hidden edges are used as validation data set, and the remaining 10% for the test set. Both sets also contain an equivalent amount of non-edges that are not in the train set. Moreover, as we also try to have a latent representation for B' , we carefully construct another validation and test set with the edges that have already been hidden for the learning of B . We compare the link prediction \widehat{B} at the observation session level (AUC1, AP1), and the link prediction \widehat{B}' at the plant-insect level (AUC2, AP2, AUC3, AP3). AUC2 and AP2 are calculated with the prediction obtained by the second latent space Z'_1, Z_2 , whereas AUC3 and AP3 are calculated from the prediction obtained by the reconstruction \widehat{B} with $\widehat{B}' = \tilde{P}^\top \widehat{B}$. Both methods are fit with 1 000 iterations of Adam algorithm with learning rate 0.005, and with a latent space of dimension 3, using a computer equipped with an Intel Xeon(R) CPU E5-1650 v4 and 32GB of RAM.

Looking at the results in Table 2, both methods have better prediction on B than on B' , and calculating $\widehat{B}' = \tilde{P}^\top \widehat{B}$ yields better results than using the second latent space. Once again the BVGAE has better AUC and AP than its fair-counterpart, however, even if the linear correlation between the latent space and the protected variable S seems low (0.051), the latent space of the BVGAE is not independent of S according to the HSIC test. Although the AUC1 decreased in average from 0.865 to 0.830, the fair-BVGAE has a latent space independent of S which is the target result: the latent representation Z_1 is independent of the users' experience levels. Looking at Figure 3 we can see a change of structure when accounting for sampling bias leading to a change of our ecological understanding of this plant-pollinator network. For example, the fair adjustment overall increases the probability of connection, notably of Lepidoptera revealing a higher contribution of butterflies to pollination. A checkerboard structure is observed for the interactions of Hymenoptera in the BVGAE suggesting contrasted preferences among plants and

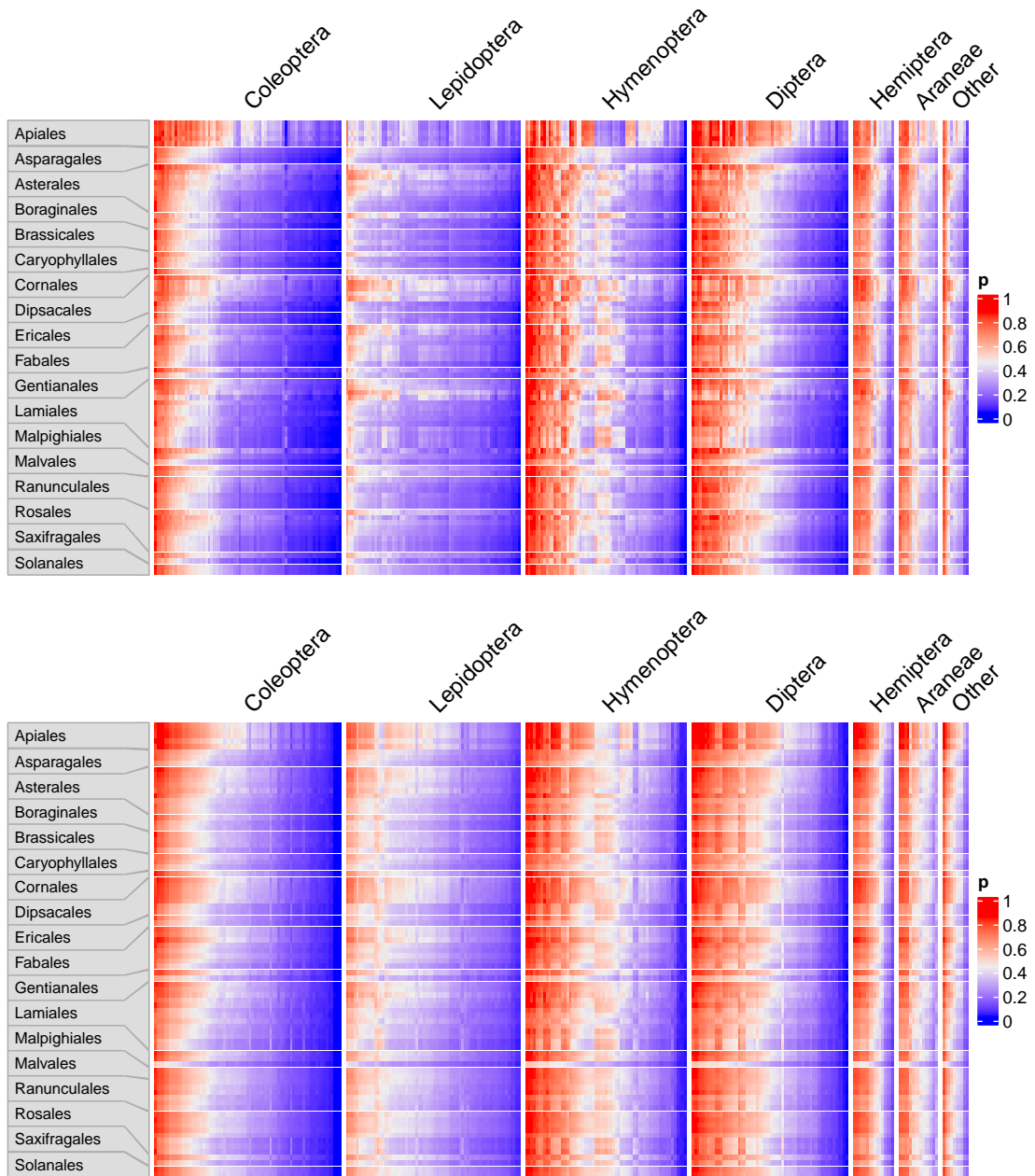


Figure 3: Estimated probabilities of connection between plants and insects on the Spipoll data set obtained with $\widehat{B}' = \tilde{P}^\top \widehat{B}$, BVGAE is on the top and the fair-BVGAE is on the bottom. Each row and column represent respectively a genus of plant and insect. However, due to the inability to plot all genus names, the insects and plants have been grouped based on their taxonomic orders. Regions in red highlight strong probability of connection, whereas regions in blue depict low probability of connection.

pollinators. This structure is smoothed in the fair-BVGAE indicating that such differences in preferences have no ecological ground but are related to the sampling process. Full representations of latent spaces are available in Appendix B.4.

6 Conclusion

In this paper, we proposed not only a bipartite extension of the graph variational auto-encoder, but also a new method to have a fair latent representation with respect to a continuous variable. Using the random Fourier Features to estimate the HSIC, our methodology is adapted to large data set. We handled a particular structure of data: observed collections of pollination events with numerous covariates from which are derived a plant-pollinator interaction network. We then used our model to tackle the sampling effects affecting this large ecological network, an issue of particular importance when the sampling involves citizen science. This methodology could provide interesting results in fields of study where both networks and sampling bias are at stake.

References

- Beel, J., B. Gipp, S. Langer, and C. Breiteringer (2016, November). Research-paper recommender systems: A literature survey. *International Journal on Digital Libraries* 17(4), 305–338.
- Botella, C., S. Dray, C. Matias, V. Miele, and W. Thuiller (2022). An appraisal of graph embeddings for comparing trophic network architectures. *Methods in Ecology and Evolution* 13(1), 203–216.
- Carey, A. N. and X. Wu (2022, March). The Fairness Field Guide: Perspectives from Social and Formal Sciences.
- Caton, S. and C. Haas (2020, October). Fairness in Machine Learning: A Survey.
- Chacoff, N. P., D. P. Vázquez, S. B. Lomáscolo, E. L. Stevani, J. Dorado, and B. Padrón (2012). Evaluating sampling completeness in a desert plant-pollinator network: Sampling a plant-pollinator network. *Journal of Animal Ecology* 81(1), 190–200.
- Cornes, R. C., G. van der Schrier, E. J. M. van den Besselaar, and P. D. Jones (2018). An Ensemble Version of the E-OBS Temperature and Precipitation Data Sets. *Journal of Geophysical Research: Atmospheres* 123(17), 9391–9409.
- Deguines, N., M. De Flores, G. Lois, R. Julliard, and C. Fontaine (2018, May). Fostering close encounters of the entomological kind. *Frontiers in Ecology and the Environment* 16(4), 202–203.
- Deguines, N., R. Julliard, M. de Flores, and C. Fontaine (2012, September). The Whereabouts of Flower Visitors: Contrasting Land-Use Preferences Revealed by a Country-Wide Survey Based on Citizen Science. *PLOS ONE* 7(9), e45822.
- Deguines, N., R. Julliard, M. de Flores, and C. Fontaine (2016). Functional homogenization of flower visitor communities with urbanization. *Ecology and Evolution* 6(7), 1967–1976.
- Doré, M., C. Fontaine, and E. Thébault (2021). Relative effects of anthropogenic pressures, climate, and sampling design on the structure of pollination networks at the global scale. *Global Change Biology* 27(6), 1266–1280.

- Durand-Bessart, C., N. J. Cordeiro, C. A. Chapman, K. Abernethy, P.-M. Forget, C. Fontaine, and F. Bretagnolle (2023). Trait matching and sampling effort shape the structure of the frugivory network in Afrotropical forests. *New Phytologist* 237(4), 1446–1462. [eprint: https://onlinelibrary.wiley.com/doi/pdf/10.1111/nph.18619](https://onlinelibrary.wiley.com/doi/pdf/10.1111/nph.18619).
- Gibson, R. H., B. Knott, T. Eberlein, and J. Memmott (2011). Sampling method influences the structure of plant—pollinator networks. *Oikos* 120(6), 822–831.
- Govaert, G. and M. Nadif (2010). Latent block model for contingency table. *Communications in Statistics—Theory and Methods* 39(3), 416–425.
- Greenfeld, D. and U. Shalit (2020, July). Robust Learning with the Hilbert-Schmidt Independence Criterion.
- Gretton, A., O. Bousquet, A. Smola, and B. Schölkopf (2005). Measuring Statistical Dependence with Hilbert-Schmidt Norms. In S. Jain, H. U. Simon, and E. Tomita (Eds.), *Algorithmic Learning Theory*, Lecture Notes in Computer Science, Berlin, Heidelberg, pp. 63–77. Springer.
- Gretton, A., K. Fukumizu, C. Teo, L. Song, B. Schölkopf, and A. Smola (2007). A kernel statistical test of independence. In J. Platt, D. Koller, Y. Singer, and S. Roweis (Eds.), *Advances in Neural Information Processing Systems*, Volume 20. Curran Associates, Inc.
- Higgins, I., L. Matthey, A. Pal, C. P. Burgess, X. Glorot, M. M. Botvinick, S. Mohamed, and A. Lerchner (2016). beta-vae: Learning basic visual concepts with a constrained variational framework. In *International Conference on Learning Representations*.
- Ings, T. C. M. e. a. (2009). Review: Ecological networks – beyond food webs. *Journal of Animal Ecology* 78(1), 253–269.
- Jiguet, F. (2009, July). Method learning caused a first-time observer effect in a newly started breeding bird survey. *Bird Study* 56(2), 253–258.
- Johnston, A., D. Fink, W. M. Hochachka, and S. Kelling (2018). Estimates of observer expertise improve species distributions from citizen science data. *Methods in Ecology and Evolution* 9(1), 88–97.
- Jordano, P. (2016). Sampling networks of ecological interactions. *Functional Ecology* 30(12), 1883–1893.
- Kalaitzis, F. and N. Lawrence (2012, June). Residual Component Analysis: Generalising PCA for more flexible inference in linear-Gaussian models. *Proceedings of the 29th International Conference on Machine Learning, ICML 2012* 1.
- Kipf, T. N. and M. Welling (2016). Variational graph auto-encoders.
- Li, P., Y. Wang, H. Zhao, P. Hong, and H. Liu (2021). On Dyadic Fairness: Exploring and Mitigating Bias in Graph Connections.
- Li, Y., H. Chen, S. Xu, Y. Ge, J. Tan, S. Liu, and Y. Zhang (2023, July). Fairness in Recommendation: Foundations, Methods and Applications.
- Li, Y., K. Liu, R. Satapathy, S. Wang, and E. Cambria (2023). Recent developments in recommender systems: A survey.

- Locatello, F., G. Abbati, T. Rainforth, S. Bauer, B. Schölkopf, and O. Bachem (2019). On the fairness of disentangled representations.
- Louizos, C., K. Swersky, Y. Li, M. Welling, and R. Zemel (2017, August). The Variational Fair Autoencoder.
- Ma, W.-D. K., J. P. Lewis, and W. B. Kleijn (2020, April). The HSIC Bottleneck: Deep Learning without Back-Propagation. *Proceedings of the AAAI Conference on Artificial Intelligence* 34(04), 5085–5092.
- Nowicki, K. and T. A. B. Snijders (2001, September). Estimation and Prediction for Stochastic Blockstructures. *Journal of the American Statistical Association* 96(455), 1077–1087.
- Rahimi, A. and B. Recht (2007, January). Random Features for Large-Scale Kernel Machines. In *Advances in Neural Information Processing Systems*, Volume 20.
- Rahman, T., B. Surma, M. Backes, and Y. Zhang (2019, August). Fairwalk: Towards Fair Graph Embedding. In *Proceedings of the Twenty-Eighth International Joint Conference on Artificial Intelligence*, Macao, China, pp. 3289–3295. International Joint Conferences on Artificial Intelligence Organization.
- Reiser, P., M. Neubert, A. Eberhard, L. Torresi, C. Zhou, C. Shao, H. Metni, C. van Hoesel, H. Schopmans, T. Sommer, and P. Friederich (2022, November). Graph neural networks for materials science and chemistry. *Communications Materials* 3(1), 1–18.
- Saxena, A., G. Fletcher, and M. Pechenizkiy (2022, September). FairSNA: Algorithmic Fairness in Social Network Analysis.
- Strydom, T., S. Bouskila, F. Banville, C. Barros, D. Caron, M. J. Farrell, M.-J. Fortin, V. Hemming, B. Mercier, L. J. Pollock, R. Runghen, G. V. Dalla Riva, and T. Poisot (2022). Food web reconstruction through phylogenetic transfer of low-rank network representation. *Methods in Ecology and Evolution* 13(12), 2838–2849.
- Sutherland, D. J. and J. Schneider (2015, June). On the Error of Random Fourier Features.
- Terry, J. C. D. and O. T. Lewis (2020). Finding missing links in interaction networks. *Ecology* 101(7), e03047.
- Tipping, M. E. and C. M. Bishop (1999). Probabilistic Principal Component Analysis. *Journal of the Royal Statistical Society: Series B (Statistical Methodology)* 61(3), 611–622.
- Veličković, P., G. Cucurull, A. Casanova, A. Romero, P. Liò, and Y. Bengio (2018, February). Graph Attention Networks.
- Wang, Y., W. Ma, M. Zhang, Y. Liu, and S. Ma (2023, July). A Survey on the Fairness of Recommender Systems. *ACM Transactions on Information Systems* 41(3), 1–43.
- Xu, K., W. Hu, J. Leskovec, and S. Jegelka (2019, February). How Powerful are Graph Neural Networks?
- Zhang, B. H., B. Lemoine, and M. Mitchell (2018, January). Mitigating Unwanted Biases with Adversarial Learning.
- Zhang, Q., S. Filippi, A. Gretton, and D. Sejdinovic (2018, January). Large-scale kernel methods for independence testing. *Statistics and Computing* 28(1), 113–130.

Zhang, X.-M., L. Liang, L. Liu, and M.-J. Tang (2021). Graph Neural Networks and Their Current Applications in Bioinformatics. *Frontiers in Genetics* 12.

A PROOFS

We note $P_S = S(S^\top S)^{-1}S^\top$ the orthogonal projection on the span of S and $P_{S^\perp} = I_d - P_S X$ the orthogonal projection on the space orthogonal to the span of S .

Proposition 1 Assume that X is centered. Let $\Lambda = \frac{1}{n}X^\top X$. Assume that X and S are jointly Gaussian. The solution of the maximization problem given by the following Lagrangian:

$$L(v) = v^\top \Lambda v + \lambda_1(1 - v^\top v) + \lambda_2 \|S^\top X v\|^2$$

can also be obtained by computing the first component of the PCA of $P_{S^\perp} X$.

Proof We can see that

$$X^\top X = (P_S X + P_{S^\perp} X)^\top (P_S X + P_{S^\perp} X) = (P_S X)^\top P_S X + (P_{S^\perp} X)^\top P_{S^\perp} X$$

and

$$\|S^\top X v\|^2 = v^\top X^\top S S^\top X v,$$

thus, we have

$$L = \frac{1}{n} v^\top (P_S X)^\top P_S X v + \frac{1}{n} v^\top (P_{S^\perp} X)^\top P_{S^\perp} X v + \lambda_1(1 - v^\top v) + \lambda_2 \|S^\top X v\|^2.$$

Derivating the Lagrangian yields

$$\frac{\partial L}{\partial v} = \frac{2}{n} (P_S X)^\top P_S X v + \frac{2}{n} (P_{S^\perp} X)^\top P_{S^\perp} X v - 2\lambda_1 v + \lambda_2 2X^\top S S^\top X v = 0, \quad (4)$$

$$\frac{\partial L}{\partial \lambda_1} = 1 - \|v\|^2 = 0, \quad \frac{\partial L}{\partial \lambda_2} = \|S^\top X v\|^2 = 0.$$

First, we can see that

$$\|S^\top X v\|^2 = 0 \implies S^\top X v = 0$$

which allows us to plug in Equation (4):

$$\frac{\partial L}{\partial v} = \frac{2}{n} (P_S X)^\top P_S X v + \frac{2}{n} (P_{S^\perp} X)^\top P_{S^\perp} X v + 2\lambda_1 v = 0. \quad (5)$$

Moreover,

$$P_S = S(S^\top S)^{-1}S^\top$$

thus

$$P_S X v = S(S^\top S)^{-1}(S^\top X v) = 0.$$

Finally, Equation (4) becomes

$$\frac{2}{n} (P_{S^\perp} X)^\top P_{S^\perp} X v - 2\lambda_1 v$$

which is equivalent to search for λ_1 and v such as

$$\frac{1}{n} (P_{S^\perp} X)^\top P_{S^\perp} X v = \lambda_1 v,$$

in other words, we are looking for the eigenvalues of the covariance matrix of X projected on S^\top , which is the same as performing a PCA on $P_{S^\perp} X$.

B EXTENSIVE SIMULATION STUDY

B.1 Impact of hyperparameter δ

We remind the expression of the variational loss given in Equation (3):

$$\begin{aligned} L = & \mathbb{E}_{q(Z_1, Z_2 | X_1, X_2, B)}[\log p(B | Z_1, Z_2)] \\ & - KL[q_1(Z_1 | X_1, B) || p_1(Z_1)] \\ & - KL[q_2(Z_2 | X_2, B) || p_2(Z_2)] \\ & + \delta RFF HSIC(\mu_1, S). \end{aligned}$$

In this expression, δ is the hyperparameter associated with the *RFF HSIC*. Setting $\delta = 0$ yields the same result as fitting the classical BVGAE. The following simulation study is performed to study the impact of this hyperparameter on the different scores.

B.1.1 Setting

The settings are nearly identical as in Section 4. In this simulation, we are going to generate bipartite networks made of $n_1 = 1000$ rows and $n_2 = 100$ columns. Let $S_i \stackrel{i.i.d.}{\sim} \mathcal{N}(0, 1)$ for $i = 1, \dots, n_1$ and $T_i \stackrel{i.i.d.}{\sim} \mathcal{N}(0, 1)$ for $i = 1, \dots, n_1$ and independent of S . We suppose that S is the protected variable. Let $Z_1 = (S, T) \in \mathbb{R}^{n_1 \times 2}$ be the 2-column matrix made with both S and T . Let $Z_2 \stackrel{i.i.d.}{\sim} \mathcal{N}\left(\begin{bmatrix} 2.5 \\ 2.5 \end{bmatrix}, \begin{bmatrix} 1 & 0 \\ 0 & 1 \end{bmatrix}\right) \in \mathbb{R}^{n_2 \times 2}$. We simulate our bipartite adjacency matrix with Bernoulli $B_{i,j} \stackrel{i.i.d.}{\sim} \mathcal{B}(\exp(-\frac{1}{2}\|Z_{1i} - Z_{2j}\|_2^2))$.

We fit the fair-BVGAE with the variational loss \mathcal{L} with hyperparameter $\delta \in \{0, 10, 100, 200, 500, 1000, 2000\}$.

B.1.2 Results

The results for the link prediction task in the simulated network are summarized in Table 3. The simulations were done with dataset splits, with 30% of the edges hidden. 20% of these hidden edges are used as validation data set, and the remaining 10% for the test set. Both sets also contain an equivalent amount of non-edges that are not in the train set. In the table are reported the mean and standard deviation for 100 trials, except for $\#p_{0.05}$ which is only a count.

For each trial, the simulations begin with 10 random initialization, and were fit using 1000 iterations of the Adam algorithm with learning rate 0.01. The model that achieved the most favorable performance on the validation test set is then selected to evaluate the performance on the test dataset.

This procedure is repeated on the same network for each value of δ .

Average and standard deviation of several metrics have been reported in Table 3. Increasing the δ parameters from 0 to 2000 decreases the *AUC* in average from 0.894 to 0.826. However, the linear correlation and the HSIC between the latent space and the protected variable decreases to reach a value closer to 0. The more δ increases, the less the independence hypothesis is rejected. Looking at Figure 4, it is also remarkable that we can reach different value for the p-value of the independence test depending on the selected value of δ .

B.2 Fair BGVAE with binary protected variable

The HSIC can encourage independence with respect to continuous variables or to categorical variables. The latter point is illustrated in this subsection.

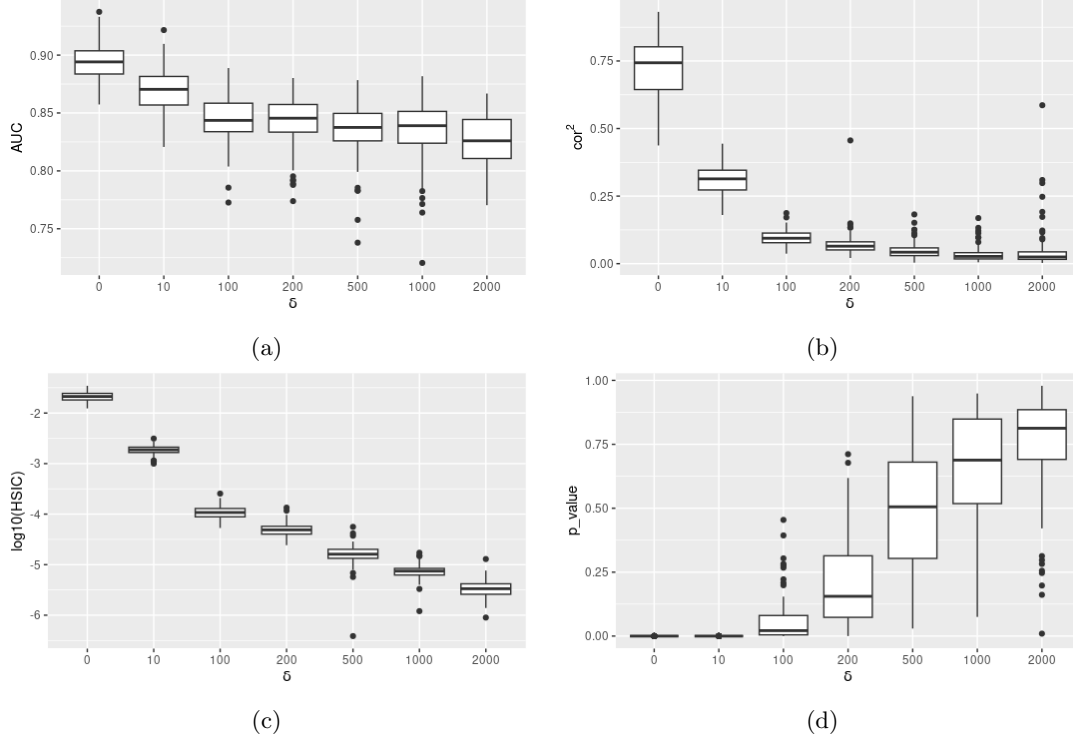


Figure 4: Impact of the parameter δ on the AUC (a), the norm of the correlation matrix (b), the \log_{10} HSIC (c), and the p-value of the independence test (d).

Table 3: Comparison of fair and bipartite variational graph auto-encoder for different value of δ on 100 trials with simulated data

δ	0	10	100	200	500	1000	2000
AUC	0.894 ± 0.016	0.870 ± 0.018	0.845 ± 0.020	0.843 ± 0.021	0.835 ± 0.024	0.834 ± 0.026	0.826 ± 0.022
AP	0.879 ± 0.021	0.848 ± 0.024	0.816 ± 0.026	0.816 ± 0.027	0.806 ± 0.031	0.807 ± 0.034	0.797 ± 0.028
HSIC	2.14×10^{-2} $\pm 0.47 \times 10^{-2}$	1.89×10^{-3} $\pm 0.39 \times 10^{-3}$	1.14×10^{-4} $\pm 0.34 \times 10^{-4}$	5.22×10^{-5} $\pm 1.82 \times 10^{-5}$	1.74×10^{-5} $\pm 0.72 \times 10^{-5}$	7.66×10^{-6} $\pm 2.44 \times 10^{-6}$	3.58×10^{-6} $\pm 1.53 \times 10^{-6}$
$\#p_{0.05}$	100/100	100/100	66/100	17/100	2/100	0 /100	1/100
cor	0.729 ± 0.108	0.311 ± 0.054	0.097 ± 0.029	0.071 ± 0.047	0.049 ± 0.031	0.035 ± 0.028	0.046 ± 0.076

B.2.1 Setting

Simulations with a similar setting as in Section 4 has been performed with a simulated latent space structured along a binary protected variable $S \in \{-1, 1\}$.

In this simulation, we are going to generate a bipartite network made of $n_1 = 1000$ rows and $n_2 = 100$ columns. Let S_i *i.i.d.* for $i = 1, \dots, n_1$ with a Rademacher distribution ($\mathbb{P}(S_i = -1) = \mathbb{P}(S_i = 1) = \frac{1}{2}$) and $T_i \stackrel{i.i.d.}{\sim} \mathcal{N}(0, 1)$ for $i = 1, \dots, n_1$ and independent of S . We suppose that S is the protected variable. Let $Z_1 = (S, T) \in \mathbb{R}^{n_1 \times 2}$ be the 2-column matrix made with both S and

T . Let $Z_2 \stackrel{i.i.d.}{\sim} \mathcal{N}\left(\begin{bmatrix} 2.5 \\ 2.5 \end{bmatrix}, \begin{bmatrix} 1 & 0 \\ 0 & 1 \end{bmatrix}\right) \in \mathbb{R}^{n_2 \times 2}$. We simulate our bipartite adjacency matrix with Bernoulli $B_{i,j} \stackrel{i.i.d.}{\sim} \mathcal{B}(\exp(-\frac{1}{2}\|Z_{1i} - Z_{2j}\|_2^2))$.

First, we fit a classical bipartite and variational graph auto-encoder on $B_{i,j}$. We expect that this auto-encoder would yield a latent representation \tilde{Z}_1 correlated with S and T . We then fit our bipartite and fair auto-encoder to compare the result and see if the yielded latent space is independent of S .

B.2.2 Results

Results for the link prediction task in the simulated network are summarized in Appendix B.2.2. The simulations were done with dataset splits, with 30% of the edges hidden. 20% of these hidden edges are used as validation data set, and the remaining 10% for the test set. Both sets also contain an equivalent amount of non-edges that are not in the train set. In the table are reported the mean and standard deviation for 100 trials, except for $\#p_{0.05}$ which is only a count. We set the hyperparameter $\delta = n_1 = 1000$. For each trial, the simulations begin with 10 random initialization, and were fit using 1000 iterations of the Adam algorithm with learning rate 0.01. The model that achieved the most favorable performance on the validation test set is then selected to evaluate the performance on the test dataset.

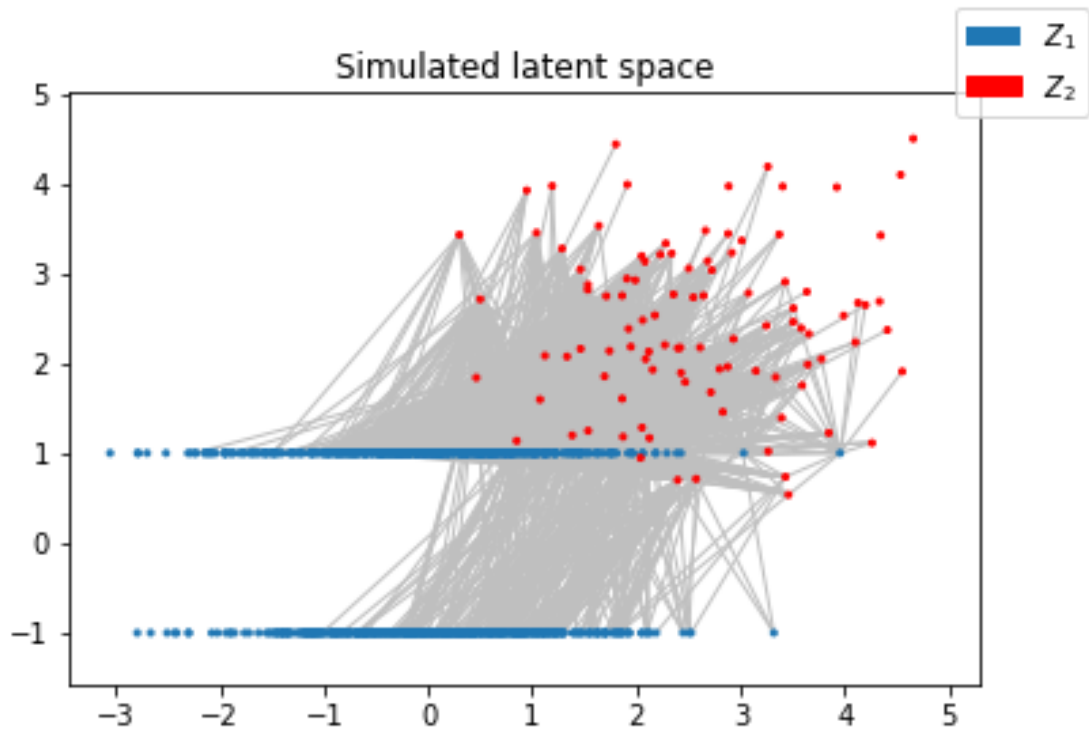


Figure 5: Simulated latent space for generating bipartite network $B_{i,j}$. $Z_1 = (T, S)$ is represented in blue. Z_2 is represented in red and is independent of Z_1 . The probability of connection between the node i and j will increase as the distance between their latent representation decreases.

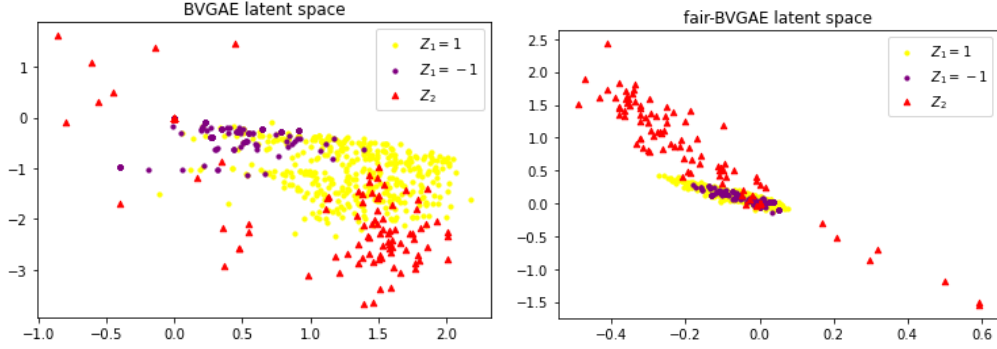


Figure 6: Estimated latent space for the bipartite variational graph auto-encoder (left) and the fair bipartite variational graph auto-encoder (right) in the binary case.

As shown in Figure 6, we are able to provide an embedding independent of the binary variable with our fair VGAE contrary to the embedding provided by the simple VGAE. Average values and standard deviation of several metrics are reported in Appendix B.2.2. As expected, the average AUC and AP decreases in the fair model compared to the classical case, however in the fair case, we do not reject the hypothesis of Independence between the latent space and the protected variable.

Table 4: Comparison between the Bipartite variational graph auto-encoder and its fair counterpart on 100 trials with binary protected variable

	BVGAE	fair-BVGAE
AUC	0.895 ± 0.016	0.831 ± 0.029
AP	0.882 ± 0.021	0.808 ± 0.038
HSIC	0.0593 ± 0.0017	$3.51 \times 10^{-6} \pm 3.08 \times 10^{-6}$
# $p_{0.05}$	100/100	0/100
cor	0.804 ± 0.112	0.020 ± 0.021

B.3 Comparison of fair linear embedding

Let $S_i \stackrel{i.i.d.}{\sim} \mathcal{N}(0,1)$ and $T_i \stackrel{i.i.d.}{\sim} \mathcal{N}(0,1)$ for $i \in 1, \dots, n = 1000$. Assume that $S \perp T$ and let $Z = (S, T)$. Let $K_{i,j} \stackrel{i.i.d.}{\sim} \mathcal{N}(0,9)$ be a 2×5 matrix. Suppose that we observe the $n \times 5$ matrix $X = ZK$ and the protected variable S .

We wish to perform a linear embedding

$$X \xrightarrow{\text{Linear}} Z \xrightarrow{\text{Linear}} \hat{X}$$

with three different methods, principal component analysis on X , principal component analysis on $P_{S^\perp}X$, and principal component analysis on X using the HSIC loss between the latent space and S as an additional loss term. This is the introductory case, where the optimal solution can be obtained with a projection. We aim to investigate if using the HSIC as a loss in this setting would yield a result similar to the optimal one.

B.3.1 Principal component analysis using X

We consider an encoder f_{W_0} with a one layer neural network of 5 input nodes and 2 output nodes, and a decoder g_{W_1} with 2 input nodes and 5 output nodes. We optimize the weights of the auto-encoder with respect to the mean squared error loss:

$$\mathcal{L}(W_0, W_1) = \frac{1}{n} \|g_{W_1}(f_{W_0}(X)) - X\|.$$

B.3.2 Principal component analysis using $P_{S^\perp} X$

We consider an encoder f_{W_0} with a one layer neural network of 5 input nodes and 2 output nodes, and a decoder g_{W_1} with 2 input nodes and 5 output nodes. We optimize the weights of the auto-encoder with respect to the mean squared error loss:

$$\mathcal{L}(W_0, W_1) = \frac{1}{n} \|g_{W_1}(f_{W_0}(P_{S^\perp} X)) - X\|.$$

The difference between the precedent model is that the encoder takes as input $P_{S^\perp} X$. In our case, this would erase all effect from the protected variable in the latent space.

B.3.3 Principal component analysis using X and the HSIC loss

We consider an encoder f_{W_0} with a one layer neural network of 5 input nodes and 2 output nodes, and a decoder g_{W_1} with 2 input nodes and 5 output nodes. We optimize the weights of the auto-encoder with respect to the MSE and HSIC loss:

$$\mathcal{L}(W_0, W_1) = \frac{1}{n} \|g_{W_1}(f_{W_0}(X)) - X\| + \delta RFF HSIC(f_{W_0}(X), S).$$

Here we have chosen $\delta = 10^5$.

For all the presented method, we fit the weights using 200 steps of the Adam algorithm with learning rate 0.01. For the HSIC loss, we fit the algorithm 10 times with different initialization before selecting the one with the lowest HSIC value. We then simulate a test set of 200 observations following the same probability law than the training test. Mean squared error, HSIC, number of time the independence hypothesis is rejected, and the Euclidean norm of the covariance between the latent space and the protected variable S are reported in Appendix B.3.3

Table 5: Comparison between the PCA, the projected PCA and the HSIC PCA

	PCA	PCA with projection	PCA with HSIC
MSE	$7.16 \times 10^{-2} \pm 21.4 \times 10^{-2}$	9.88 ± 6.34	8.80 ± 5.54
HSIC	3.15×10^{-2} $\pm 1.02 \times 10^{-2}$	1.15×10^{-3} $\pm 0.60 \times 10^{-3}$	2.21×10^{-3} $\pm 4.81 \times 10^{-3}$
$\#p_{0.05}$	100/100	3/100	10/100
cor	0.991 ± 0.229	$6.83 \times 10^{-2} \pm 4.92 \times 10^{-2}$	0.142 ± 0.241

Removing the protected variable S from the original data X has increased the MSE, which was the expected behavior because X depends on S . However, doing the projection or adding the HSIC as a penalty term in the loss have yielded results where the latent space became independent of the protected variable. Looking at Figure 7 we can see an example where the latent space of the PCA with projection and the PCA with HSIC are similar.

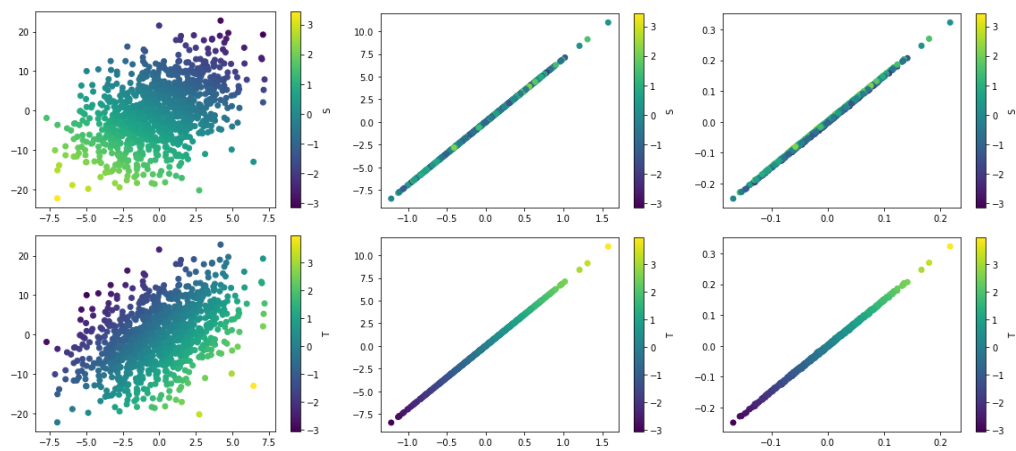


Figure 7: Latent representation of the linear embedding performed on X (left), performed on $P_{S^\perp} X$ (middle), and performed on X with the HSIC loss (right). The latent space is colored according to the protected variable S (top) and the variable T (bottom). Adding the HSIC as a loss term yielded similar latent space as making the embedding on $P_{S^\perp} X$, except that the points are not perfectly aligned.

B.4 Spipoll, exploration with higher dimensional latent spaces

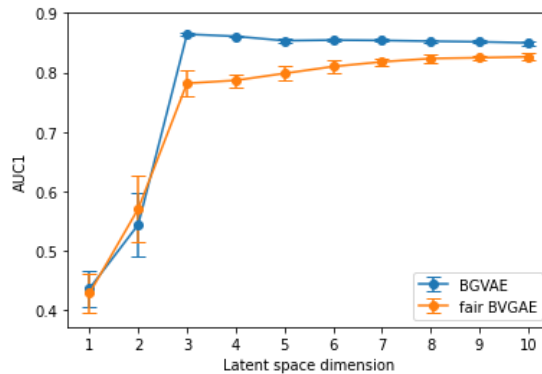


Figure 8: Estimated mean and 95% confidence intervals for the AUC1 for link prediction in the Spipoll data set using BGVAE and the fair BGVAE for various latent space size.

In Section 5.3 we show in detail the results for the case where the latent space has 3 dimensions. We justify this choice by looking at the estimated mean of the AUC1 for different number of dimension for the latent space. Looking at Figure 8, we can see that the most favorable case for the BGVAE is when the dimension is equal to 3. For the fair-BVGAE, the AUC keeps increasing for higher number of dimensions.

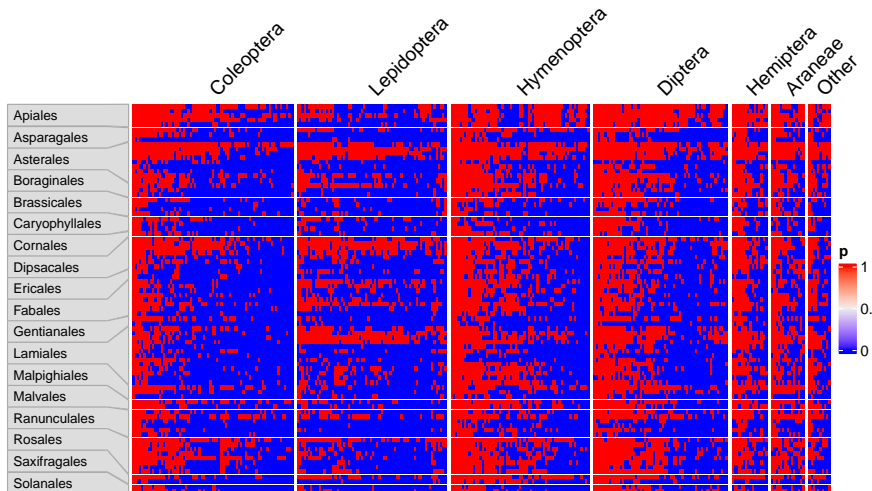


Figure 9: Observed initial plant-insect network

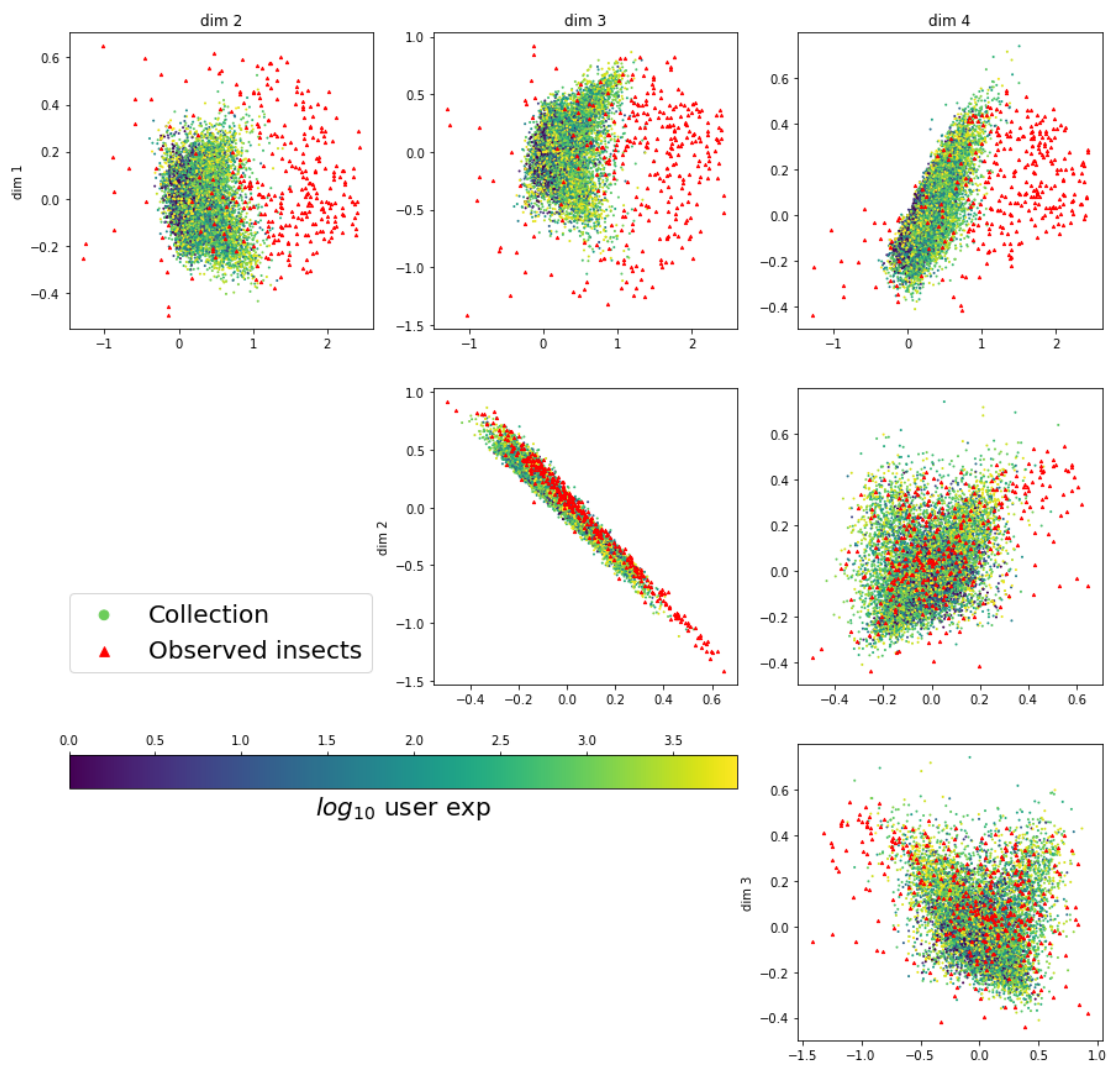


Figure 10: Estimated latent space for the Spipoll data set using BVGAE

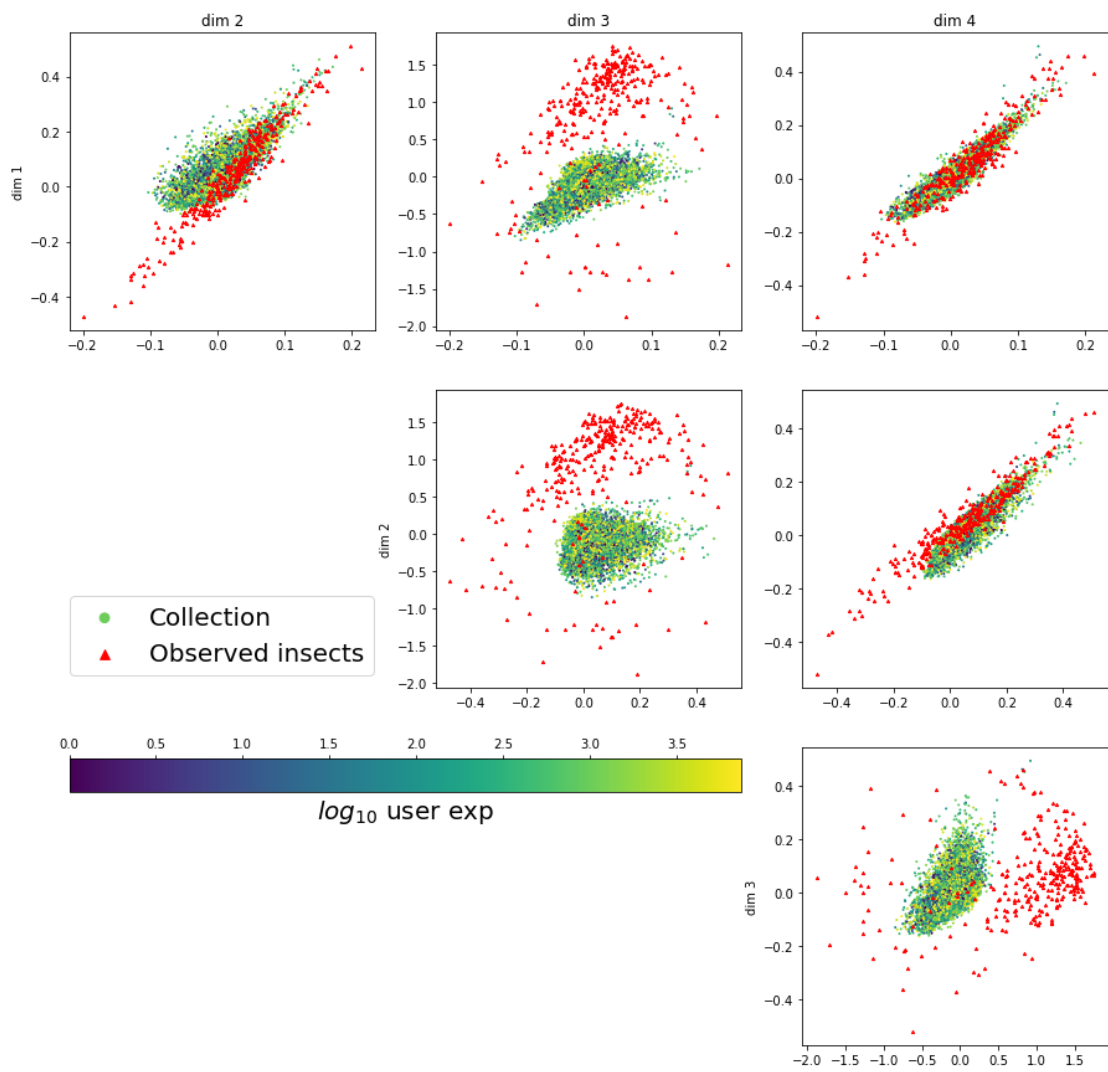


Figure 11: Estimated latent space for the Spipoll data set using fair-BVGAE